Cerebellar Blood Flow and Metabolism in Cerebral Hemisphere Infarction

W. R. Wayne Martin, MD, and Marcus E. Raichle, MD

Positron emission tomography was used to study the effect of supratentorial infarction on cerebellar metabolic rate for oxygen and cerebellar blood flow. In a control group of patients, the mean cerebellar metabolic rate for oxygen was 2.97 ± 0.11 (standard error of the mean [SEM]) $ml^{-1} \cdot min^{-1} \cdot hg^{-1}$ and mean cerebellar blood flow was 41.1 ± 1.5 $ml \cdot min^{-1} \cdot hg^{-1}$. No significant right-left asymmetry in either cerebellar metabolic rate for oxygen or cerebellar blood flow was noted. Patients with frontal lobe infarction showed 16.8 ± 1.8% (cerebellar metabolic rate for oxygen) and 19.6 ± 2.1% (cerebellar blood flow) differences between cerebellar hemispheres, with the hemisphere contralateral to the cerebral infarction having the lower values. These differences were highly significant ($p < 0.001$). In addition, cerebellar blood flow and cerebellar metabolic rate for oxygen were significantly decreased in the ipsilateral cerebellar hemisphere (metabolism: 2.13 ± 0.19 $ml \cdot min^{-1} \cdot hg^{-1}$; $p < 0.002$; blood flow: 35.2 ± 2.4 $ml \cdot min^{-1} \cdot hg^{-1}$; $p < 0.05$). Patients with parietooccipital infarction also showed a significant bilateral decrease in cerebellar metabolic rate for oxygen (2.43 ± 0.11 $ml \cdot min^{-1} \cdot hg^{-1}$) and cerebellar blood flow (34.6 ± 2.5 $ml \cdot min^{-1} \cdot hg^{-1}$) relative to control subjects, but no significant cerebellar asymmetry. Our findings demonstrate a general depression of cerebellar blood flow and metabolism from cerebral hemisphere infarction unrelated to the site of infarction as well as a specific depression occurring contralateral to infarction involving the frontal lobe. These are among the first quantitative data concerning regional cerebellar metabolic rates for oxygen and cerebellar blood flow in humans.

Martin WRW, Raichle ME: Cerebellar blood flow and metabolism in cerebral hemisphere infarction. Ann Neurol 14:168–176, 1983

Acute hemispheric cerebral infarction is known to be associated with impairment of regional hemodynamics and metabolism in areas of the brain remote from the infarcted tissue. These effects have been noted in the cerebral hemisphere contralateral to the infarction [9, 12, 17, 19, 20, 26] as well as in the contralateral cerebellar hemisphere [2, 3, 17]. Reports concerning these findings in the cerebellum [2, 3, 17], all thus far in abstract form, have dealt only with relative asymmetries in cerebellar hemispheres and have not given quantitative values for cerebellar blood flow or metabolism.

Using positron emission tomography (PET), we have quantified the regional cerebral blood flow (CBF), the regional cerebellar blood flow (CbBF), the cerebral metabolic rate for oxygen ($CMRO_2$), and the cerebellar metabolic rate for oxygen ($CbMRO_2$) in patients with hemispheric cerebral infarction. We have examined the relationship between infarcts in specific regions of the cerebral hemispheres and CbBF and $CbMRO_2$ to better understand the critical spatial and temporal factors involved.

Methods

The scans of all patients with x-ray computed tomographic (CT) evidence of cerebral infarction who had positron emission tomography at Washington University's Barnes Hospital were reviewed. These patients were a selected group with minor neurological deficits who were being considered for extracranial-intracranial (EC-IC) bypass (superficial temporal to middle cerebral artery anastomosis). Patients with major neurological deficits (such as hemiplegia or aphasia) were not included. Those with clinical or CT evidence of posterior fossa involvement were also excluded, as were patients with subarachnoid hemorrhage and those in whom the cerebellum was not adequately imaged. The study group consisted of 16 patients who had a total of twenty-five measurements of blood flow and metabolism. Seven patients had repeat studies following EC-IC bypass.

A control group consisted of patients with psychiatric depressive illnesses who were considered candidates for electroconvulsive therapy. This group comprised 7 patients who had a total of ten measurements of metabolism and eleven measurements of blood flow. Four patients had repeat studies following electroconvulsive therapy.

PET was performed with the PETT VI system [28]. Design and performance characteristics have been discussed

From The Edward Mallinckrodt Institute of Radiology, The McDonnell Center for Studies of Higher Brain Function, and the Department of Neurology and Neurosurgery, Washington University School of Medicine, St. Louis, MO 63110.

Received Aug 6, 1982, and in revised form Dec 27, 1982. Accepted for publication Jan 2, 1983.

Address reprint requests to Dr Raichle, Box 8131, Washington University School of Medicine, 510 S Kingshighway, St. Louis, MO 63110.

elsewhere [28, 34]. Data are recorded simultaneously from seven slices with a center-to-center separation of 14.4 mm. All studies were done in the low-resolution mode, giving an in-plane (that is, transverse) resolution of 11.7 mm full width at half maximum at the center of the field of view and a slice thickness of 13.9 mm full width at half maximum at the center.

Patient preparation included the percutaneous insertion of a radial artery catheter under local anesthesia to permit frequent sampling of arterial blood, and the insertion of an intravenous catheter for isotope injection in the opposite arm. The head was positioned with the aid of a vertical laser line so that the center of the lowest slice corresponded to the patient's orbitomeatal line. A lateral skull roentgenogram with this line marked by a vertical radiopaque wire provided a permanent record of the patient's exact position in relation to the lowest PET slice. A molded plastic face mask prevented major head movements during the scan [28]. This system enables accurate repositioning in patients undergoing sequential studies. After the head was in place, a transmission scan was performed with a ring phantom containing germanium 68 for attenuation correction. During the PET scans the room was darkened and patients were instructed to keep the eyes closed. The ears were not occluded. Ambient room noise during the scans consisted almost entirely of noise from the cooling fans for the electronic equipment.

For the measurement of regional CBF and CbBF, an emission scan (scan length, 40 seconds) was performed following an intravenous bolus injection of 12 ml of saline containing 50 to 100 mCi of oxygen 15 water (half-life, 124 seconds). Arterial blood samples were drawn about every five seconds during the scan. These samples were weighed and counted in a well counter to obtain the activity of ^{15}O in each sample (counts per second per gram of blood), and this activity was corrected for the physical decay of ^{15}O from the time of injection to the time of measurement. A curve of the decay-corrected blood activity as a function of time was constructed. Calibration of the tomograph to obtain the actual regional isotope concentration in the brain from the reconstructed image (counts per second per milliliter of tissue) was performed by imaging a phantom divided into six wedge-shaped chambers of equal size. The chambers were filled with varying concentrations of carbon 11 bicarbonate. Aliquots from each chamber were counted in the same well counter used for the measurement of blood radioactivity, and the observed counting rate was decay corrected to the time scanning of the phantom commenced. From these data (counts·ml^{-1}·sec^{-1}; $C_{initial}$), the total number of counts (counts per milliliter; C_{total}) presented to the scanner during the length of the scan was obtained by integrating the exponential decay curve over the length of the scan (T_1) in the following manner:

$$C_{total} = \int_0^{T_1} C_{initial} \exp(-\lambda t)dt = \text{counts/ml}$$

where λ is the decay constant for the isotope (ie, 0.693/isotope half-life). After the phantom image was reconstructed, a regression equation was obtained comparing the relative scan data and the directly measured activity from the phantom. From this relationship the actual local isotope concentrations can be obtained from each subject's scan.

Because our scanner does not correct for radioactive decay during data collection, it is necessary to correct PETT VI patient scan data for the isotope decay that occurs during the study. The method we employ is derived by assuming a function of activity that would be constant were it not for decay. This is equivalent to computing the average decay over the interval T, that is:

$$\text{average decay} = \int_0^T \exp(-\lambda T)dt/T = \frac{1 - \exp(-\lambda T)}{\lambda T}$$

Inversion of the average decay yields an "average" decay correction. Simulation studies (unpublished observations, W. R. W. Martin, M. E. Raichle) of various functions equivalent to time-varying head activity curves likely to be encountered during our patient studies demonstrate that this method of decay correction is adequate (maximum error less than 4%).

The blood curve and scan data were analyzed according to general principles of inert gas exchange developed by Kety [14] and later embodied in a tissue autoradiographic technique for the measurement of regional brain blood flow in laboratory animals [16, 24]. With this method the regional cerebral blood flow is obtained by numerically solving the following equation for f, the flow per unit weight of tissue:

$$C_i(T) - fC_A(t)*\exp(-f/\lambda t)$$

where $C_i(T)$ is the local radiotracer concentration at time T, derived from a quantitative autoradiogram of a brain slice; $C_A(t)$ is the measured concentration of radiotracer in arterial blood as a function of time and is the brain/blood equilibrium partition coefficient for the tracer. The operation of convolution is denoted by the midline asterisk. PET scanners, including the one employed in this study [28], do not have adequate temporal resolution to measure tissue radioactivity ($C_i(T)$) instantaneously. Thus, to employ the autoradiographic technique for in vivo human studies, a scan must be performed over many seconds, essentially summing the instantaneous tissue radioactivity over time. We have therefore modified the operational equation for this model (presented earlier) by an additional integration over the time of the scan ($T_2 - T_1$; 40 seconds [22]), as follows:

$$C = \int_{T_1}^{T_2} C_i(t)dt = f\int_{T_1}^{T_2} C_A(t)*\exp(-f/\lambda t)dt$$

where C is the local tissue activity measured by PET. To establish the validity of this technique, we have measured local CBF with PET in a single cerebral hemisphere of adult baboons anesthetized with nitrous oxide and compared it directly with blood flow measured in the same cerebral hemisphere using the internal carotid artery injection of ^{15}O water and standard tracer principles [7]. The details of these validation experiments will be reported separately. The correlation between the PET-measured CBF and the true CBF for the same cerebral hemisphere was excellent. Over a blood flow range of 10 to 63 ml · min^{-1} · hg^{-1}, CBF(PET) = 0.90 CBF(true) + 0.40 ($n = 23$, $r = 0.96$, $p < 0.001$). The slight underestimation of CBF(true) by CBF(PET) is caused by the brain permeability limitation of ^{15}O water. Because the brain

permeability for water is less in the baboon than in humans (unpublished observations, W. R. W. Martin, M. E. Raichle), we believe the underestimation of CBF in data presented in this study to be minimal (i.e., less than 5%).

The measurement of the local cerebral and cerebellar metabolic rate for oxygen was achieved by adapting a method originally developed in our laboratory for the measurement of oxygen utilization [27] and which we have previously validated [21]. Details are to be published, but we present here a brief summary of this method and the results of our validation studies. The original technique required the sequential intracarotid injection of two aliquots of the subjects' blood labeled first with ^{15}O oxyhemoglobin and second with ^{15}O water. From these data we computed the CBF and the local extraction of oxygen (E). Combining the CBF and E with the arterial concentration of oxygen ($[O_2]$) permitted the calculation of the $CMRO_2$ (ie, $CMRO_2 = CBF \times E \times [O_2]$). In a PET extension of this technique, we administer the ^{15}O oxygen by inhalation of a single breath of air containing 50 to 100 mCi of $O^{15}O$. A PET scan is obtained immediately following the inhalation (scan length, 40 seconds), and arterial blood radioactivity is monitored from the time of inhalation through the completion of the scan (total study length, 1 minute). Whereas in the original method [21, 27] the local oxygen extraction (E) was obtained directly from the clearance curve resulting from the intracarotid injection of ^{15}O oxyhemoglobin, our PET extension of the technique uses the relationship between the extravascular tissue radioactivity obtained with $O^{15}O$ administered by inhalation and that obtained with $H_2{}^{15}O$ administered intravenously. Scan data are corrected for radioactivity in the vascular compartment by determining the local cerebral blood volume as described by Grubb and colleagues [8], using inhaled ^{15}O carbon monoxide as the tracer, and subtracting the product of the local cerebral blood volume and the blood radioactivity subsequent to the administration of $O^{15}O$ and $H_2{}^{15}O$ from their respective PET scan data. The model accounts for the fact that brain intravascular radioactivity differs from the activity measured in a peripheral artery (radial artery) because of the tissue extraction of the tracer. We account for the presence of recirculating ^{15}O water of metabolism in our arterial blood samples by measuring it directly in fractionated samples of plasma. The product of E, CBF, and arterial oxygen content gives the local $CMRO_2$ in $ml \cdot min^{-1} \cdot hg^{-1}$.

To establish the validity of this extension of our original method for the measurement of the $CMRO_2$, we measured the brain extraction of oxygen (E) in adult baboons with PET and compared it with the simultaneous measurement of E determined by both the measurement of arterial and venous (jugular bulb) oxygen content differences and the original intracarotid technique [21, 27] using ^{15}O blood. The correlation between PET-measured E and the true E for the same cerebral hemisphere was excellent: $E(PET) = 1.04\ E(true) + 0.02$ ($n = 22$, $r = 0.98$, $p < 0.001$).

The total absorbed radiation dose, if the maximum dose (100 mCi) of each of these three compounds is administered, is 490 mrem for the whole body. The critical organs are the tracheal mucosa, which receives 3,100 mrem, and the blood, which receives 2,400 mrem.

The calculations for regional blood flow, oxygen consumption, and blood volume were performed for each pixel of the reconstructed image. A region of interest 13.5 mm^2 in size was selected in each lateral cerebellar region such that the region of interest was centered around the area of maximum $CMRO_2$ and was in the contralateral area symmetrical to the infarcted zone. The average $CMRO_2$ in each region of interest and the percent difference between sides was recorded. The same region of interest was obtained on the CBF scans, and the average CBF and percent differences were recorded in a similar fashion.

These studies were approved by the Human Studies Committee and the Radioactive Drug Research Committee (United States Food and Drug Administration) of the Washington University School of Medicine. Informed consent was obtained from each patient prior to PET scanning.

Results

The control group consisted of 7 patients who underwent ten measurements of oxygen consumption and eleven measurements of blood flow. The calculated $CbMRO_2$ in the lateral cerebellar region was $2.97 \pm 0.11\ ml \cdot min^{-1} \cdot hg^{-1}$ (mean ± SEM). The degree of asymmetry between sides was 3.7 ± 0.88% (mean ± SEM). Calculated CbBF in the same regions was 41.1 ± 1.5 $ml \cdot min^{-1} \cdot hg^{-1}$ with 3.2 ± 0.73% asymmetry between sides. These side-to-side asymmetries were insignificant (Mann-Whitney rank-sum test). The partial pressure of arterial carbon dioxide was 33 ± 0.7 mm Hg (mean ± SEM).

A total of twenty-five PET studies in 16 patients with cerebral infarction were reviewed. Thirteen patients (seventeen measurements of oxygen consumption and twenty-one measurements of blood flow) were suitable for cerebellar quantitation. The delay between time of onset of infarction and PET ranged from five days to 30 months. The infarcted area included the frontal lobes in 10 patients (twelve measurements of oxygen consumption and sixteen measurements of blood flow) and was limited to the parietooccipital region in 3 patients (five measurements of blood flow and metabolism). Clinical data are listed in Table 1.

Marked cerebellar functional asymmetry characterized all patients with frontal lobe infarction. The results are listed in Table 2. The cerebellar hemisphere with the lower $CbMRO_2$ and CbBF was contralateral to the cerebral infarction in all cases. The degree of $CbMRO_2$ asymmetry was 16.8 ± 1.8% (mean ± SEM) and of CbBF asymmetry 19.6 ± 2.1% (mean ± SEM). These differences are highly significant in comparison with values in the control group for both $CbMRO_2$ and CbBF ($p < 0.001$, Mann-Whitney rank-sum test). In the patient group the mean $CbMRO_2$ for the ipsilateral cerebellar hemisphere was $2.13 \pm 0.19\ ml \cdot min^{-1} \cdot hg^{-1}$ and the mean CbBF was $35.2 \pm 2.4\ ml \cdot min^{-1} \cdot hg^{-1}$. These values differ significantly from those in the control group ($p < 0.002$ for $CbMRO_2$ and $p < 0.05$ for CbBF, Mann-Whitney rank-sum test). There was no observable relationship between the degree of asymmetry and the elapsed time from onset of infarc-

Table 1. Patient Data

Patient No.	Sex; Age (yr)	Infarct Location	Time since Infarction	Severity of Motor Deficit
1 A[a]	F; 49	L posterior frontal	6 wk	Mild
B			14 wk	Mild
2 A[a]	F; 50	L anterior frontal	12 wk	Mild
B			14 wk	Mild
3 A[a]	M; 54	L posterior frontal	20 wk	Very mild
B			26 wk	Very mild
4	M; 53	R frontoparietal	5 days	Moderate
5	M; 50	R basal ganglia, insula	7 days	Mild
6 A[a]	M; 61	R posterior frontal	17 days	Moderate
B			40 days	Moderate
7	F; 68	R frontoparietal	44 days	Moderate
8	M; 55	R posterior frontal	51 days	Very mild
9 A[a]	M; 65	R posterior frontal	18 mo	Mild
B			18.5 mo	Mild
10 A[a]	M; 48	R frontotemporo-	2 yr	Mild
B		parietal	2.04 yr	Mild
11 A[a]	F; 64	L parietooccipital	13 days	Mild
B			4 wk	Mild
C			7 mo	Mild
12	F; 42	L parietal	30 mo	Mild
13	M; 56	R parietooccipital	3 wk	Nil

[a]Before extracranial-intracranial bypass; subsequent scan(s) after bypass.

F = female; M = male; L = left; R = right.

Table 2. Cerebellar Blood Flow and Oxygen Consumption in Patients with Frontal Lobe Infarction

	CbBF(ml · min^{-1} · hg^{-1})			$CbMRO_2$(ml · min^{-1} · hg^{-1})		
Patient No.	Ipsi.[a]	Contra.[b]	Asymmetry (%)	Ipsi.[a]	Contra.[b]	Asymmetry (%)
1 A[c]	44.0	36.0	18.2	3.04	2.56	15.7
B	38.2	36.9	3.4	2.31	2.43	5.2
2 A[c]	45.0	39.6	12.0	2.11	1.81	14.2
B	29.0	26.4	9.0	1.42	1.25	12.0
3 A[c]	35.4	25.5	27.9	1.97	1.54	21.8
B	32.6	24.8	23.9	3.18	2.44	23.3
4	36.5	30.1	17.5	...	...	...
5	57.1	41.7	27.0	...	...	...
6 A[c]	30.0	27.2	9.3	1.70	1.52	10.6
B	23.8	21.2	10.9	1.73	1.42	17.9
7	24.4	17.5	28.3	1.26	0.93	26.2
8	44.0	35.4	19.5	2.53	2.16	14.6
9 A[c]	25.5	21.2	16.9	2.52	2.02	19.8
B	34.5	27.7	19.7	...	...	...
10 A[c]	22.8	14.0	38.6	1.27	1.06	16.5
B	40.7	26.5	34.9	...	...	...
Mean	35.2	28.3	19.7	2.13	1.79	16.8
SEM	2.4	2.0	2.4	0.19	0.16	1.8
Control group						
Mean	41.1[d]		3.2	2.97[d]		3.7
SEM	1.5		0.7	0.11		0.9

[a]Cerebellar hemisphere ipsilateral to cerebral infarction.
[b]Cerebellar hemisphere contralateral to cerebral infarction.
[c]Before extracranial-intracranial bypass; subsequent scan(s) after bypass.
[d]Mean for both cerebellar hemispheres.

CbBF = cerebellar blood flow; $CbMRO_2$ = cerebellar metabolic rate for oxygen; SEM = standard error of the mean.

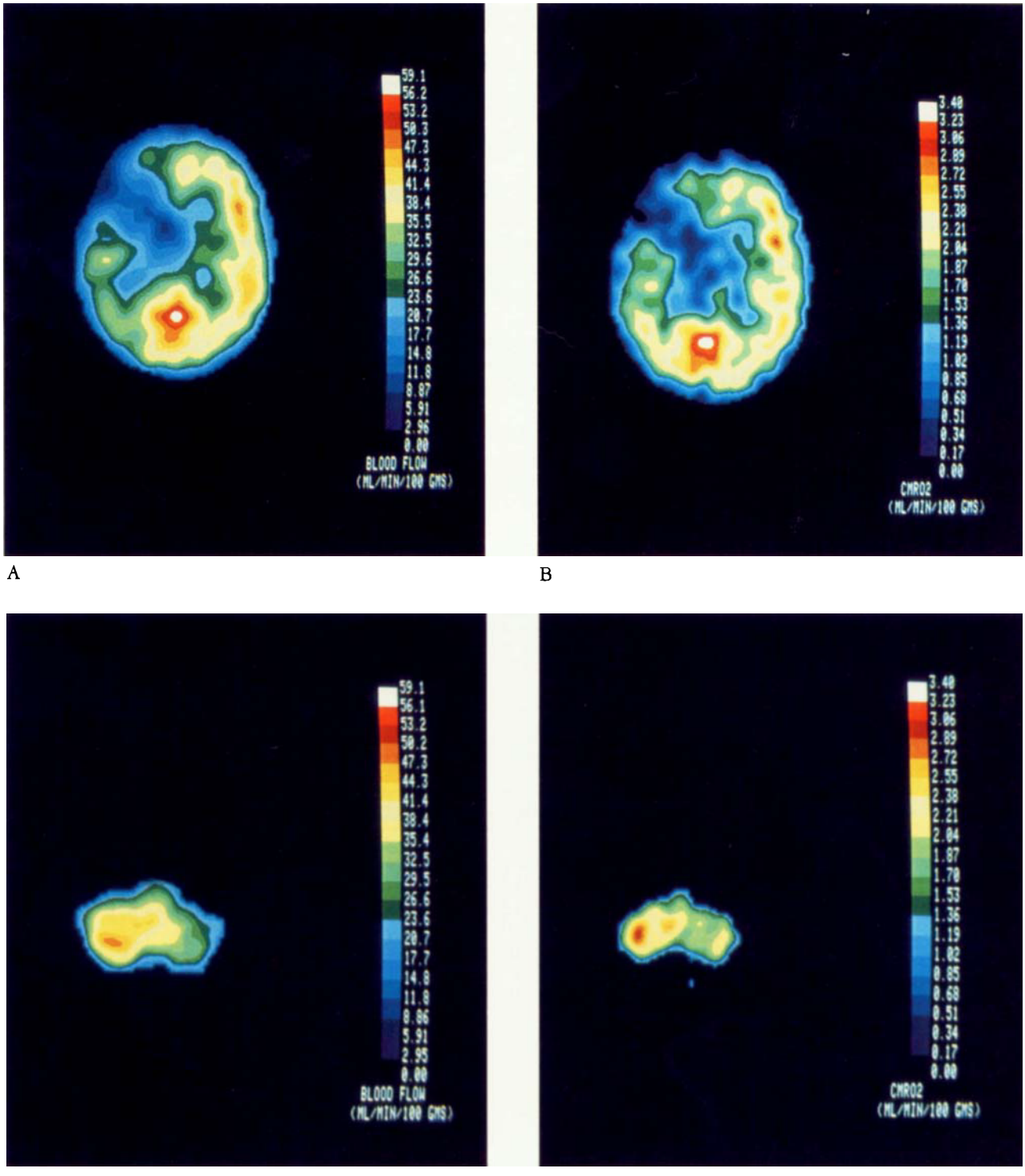

A B

C D

A typical example (patient 3A, Table 2) of crossed cerebellar diaschisis in a patient with a left frontal infarct. The cerebral blood flow and metabolic rate for oxygen are shown in (A) and (B) respectively. The area of infarction is seen as a large area of markedly reduced blood flow and oxygen consumption. The cerebellar blood flow and metabolic rate for oxygen are seen in (C) and (D) respectively. Note the reduced blood flow and oxygen consumption in the right cerebellar hemisphere. These images are oriented such that anterior is up and left is to the reader's left.

Table 3. Cerebellar Blood Flow and Metabolism in Patients with Parietal and/or Occipital Infarction Only

Patient No.	CbBF (ml · min^{-1} · hg^{-1})			CbMRO$_2$(ml · min^{-1} · hg^{-1})		
	Ipsi.[a]	Contra.[b]	Asymmetry (%)	Ipsi.[a]	Contra.[b]	Asymmetry (%)
11 A[c]	30.6	32.5	5.8	2.52	2.66	5.3
B	36.2	37.5	3.5	2.14	2.18	1.8
C	33.1	35.9	7.8	2.81	2.84	1.1
12	46.5	46.3	0.4	2.69	2.64	1.9
13	24.2	23.6	2.5	1.89	1.97	4.1
Mean	34.1	35.2	4.0	2.41	2.46	2.8
SEM	3.7	3.7	1.3	0.17	0.16	0.8
Control group						
Mean	41.1[d]		3.2	2.97[d]		3.7
SEM	1.5		0.7	0.11		0.9

[a]Cerebellar hemisphere ipsilateral to cerebral infarction.
[b]Cerebellar hemisphere contralateral to cerebral infarction.
[c]Before extracranial-intracranial bypass; subsequent scan(s) after bypass.
[d]Mean for both cerebellar hemispheres.

CbBF = cerebellar blood flow; CbMRO$_2$ = cerebellar metabolic rate for oxygen; SEM = standard error of the mean.

Table 4. Degree of Cerebral and Cerebellar Asymmetry before and after Extracranial-Intracranial Bypass in Patients without Cerebral Infarction

Patient No.; Sex; Age (yr)	Ischemic Region	Before or after Bypass	Cerebral Asymmetry (%)				Cerebellar Asymmetry (%)			
			CMRO$_2$		CBF		CbMRO$_2$		CbBF	
16; M; 70	Right MCA distribution	Before	R < L	26.5	R < L	26.7	R < L	0.8	R < L	0.6
		After	R < L	8.2	R < L	8.9	L < R	4.8	R < L	2.7
17; F; 55	Right MCA distribution	Before	R < L	9.3	R < L	15.1	L < R	8.7	L < R	6.0
		After	R < L	8.1	L < R	5.7	L < R	3.2	L < R	4.6

CMRO$_2$ = cerebral metabolic rate for oxygen; CBF = cerebral blood flow; CbMRO$_2$ = cerebellar metabolic rate for oxygen; CbBF = cerebellar blood flow; M = male; F = female; MCA = middle cerebral artery; R = right; L = left.

tion to PET scan, the severity of motor impairment, or the size of cerebral infarction. A scan from a typical patient from this group is shown in the Figure.

Six patients with frontal lobe infarction were studied both before and after EC-IC bypass. Although in one of these patients a marked improvement in CbMRO$_2$ and CbBF symmetry was noted after bypass, no statistically significant change in either symmetry or absolute values was evident for the group (Wilcoxon's signed-rank test). There was no significant change in CMRO$_2$ or CBF in either infarcted or noninfarcted tissue following bypass in these patients.

Three patients studied had parietooccipital infarction only and minimal or no motor deficit on clinical examination. The results from these patients are listed in Table 3. The associated degree of cerebellar asymmetry was not significantly different from that of the control group (Mann-Whitney rank-sum test). The mean CbMRO$_2$ and CbBF (the two cerebellar hemispheres combined) were 2.43 ± 0.11 ml · min^{-1} · hg^{-1} and 34.6 ± 2.5 ml · min^{-1} · hg^{-1}, respectively. These values differ significantly from those in the control group ($p < 0.01$ for CbMRO$_2$ and $p < 0.05$ for CbBF, Mann-Whitney rank-sum test) but do not differ from the values obtained from the cerebellar hemisphere ipsilateral to the frontal infarction (see Table 2).

The results from 2 patients with decreased CMRO$_2$ and CBF in the distribution of an occluded internal carotid artery but without clinical or CT evidence for cerebral infarction are listed in Table 4. Both CMRO$_2$ and CBF studies were repeated after EC-IC bypass, and there was marked improvement in cerebral hemisphere metabolism and blood flow. The degree of cerebellar asymmetry before bypass did not differ significantly from that of the control group (Mann-Whitney rank-sum test), and there was n postsurgical change.

Discussion

Errors associated with quantitation of small objects with PET are recognized [10, 18]. These errors are most prominent for objects with a size less than twice the instrument resolution (full width at half maximum). The cerebellar weight in the average male is 150 gm

[33]. Assuming a density similar to water, the volume of each cerebellar hemisphere is 50 to 75 cm^3. This is well above the critical volume, considering our resolution of 11.7 mm full width at half maximum and slice thickness of 13.9 mm [28]. The region of interest for $CbMRO_2$ and CbBF calculation was placed visually in the zone of highest metabolism, which tended to be in the lateral part of the hemisphere. Therefore, these measurements are for a mixture of cerebellar cortex, cerebellar white matter, and, to a lesser extent, the dentate nucleus.

The selection of patients with depressive illnesses for the control group deserves comment. The effects of depression and of electroconvulsive therapy on cerebral blood flow and metabolism are largely unknown. There is no evidence to suggest that cerebellar values are affected, however, either symmetrically or asymmetrically. Both the absolute values for CbBF and $CbMRO_2$ and the degree of asymmetry seen in our control group fall within the range seen in the few true normal subjects we have studied (n = 4).

The concept that a transient depression of function can occur at a distance from a focal cerebral lesion was formulated by von Monakow in 1914 [32], who termed the phenomenon *diaschisis*. In 1958 Kempinsky showed that a transient depression in cortical electrical activity occurred contralateral to a focal cortical lesion and that this effect depended on the presence of an intact corpus callosum [11]. He proposed a unified concept for the development of diaschisis. This concept holds that the activity of one neuronal group is facilitated by the constant input of impulses from a second group. If this second group is then destroyed, the first is deprived of one of its usual sources of facilitation and becomes less active. Eventually it assumes greater autonomy and functions at a level approaching normal. In normal brain, local CBF is regulated by regional metabolic activity [23]. Decreased neuronal activity results in a measurable decrease in $CMRO_2$ and CBF. Based on the concept of diaschisis put forth by Kempinsky [12], measurements of CBF and $CMRO_2$ should permit the detection of regions of diaschisis.

Many investigators have observed reduction in CBF in the cerebral hemisphere contralateral to cerebral infarction [9, 12, 17, 19, 20, 26]. PET has permitted a more precise demonstration of such regional effects occurring remote from the site of infarction. Kuhl and colleagues [15] showed decreased glucose metabolism in the noninfarcted ipsilateral thalamus in patients with infarction in the middle cerebral artery distribution. They also showed decreased metabolism in visual cortex that appeared normal on transmission CT scan in 2 patients with homonymous hemianopia secondary to middle cerebral artery distribution infarction [15]. Lenzi and co-workers [17] showed decreased CBF and $CMRO_2$ in the nonischemic cerebral hemisphere in 50% of their patients with cerebral infarcts. In half of the affected patients, this decrease was localized to the contralateral area homologous to the infarcted zone.

It is known that extensive unilateral cerebral hemispheric lesions occurring early in life may lead to Purkinje and granular cell degeneration in the opposite cerebellar hemisphere [31]. These changes may be associated with macroscopic unilateral cerebellar atrophy. One of the first in vivo observations in adult humans that cerebral hemisphere damage causes changes in cerebellum was reported by Baron and colleagues [2, 3], who observed a decrease in blood flow and oxygen extraction in the cerebellar hemisphere contralateral to a cerebral infarct. They observed qualitative cerebellar asymmetries only in patients with considerable hemiparesis and not in those with minimal hemiparesis. The presence of crossed cerebellar diaschisis was, however, not related to the size of cerebral infarction and was not observed later than 2 months after infarction. Lenzi and co-workers [17] also mentioned the presence of crossed cerebellar diaschisis in patients with cerebral hemispheric infarction. In contrast to Baron and colleagues [2, 3], they noted that the reduction in cerebellar flow and metabolism appeared to increase with time. Lenzi and co-workers [17] further mentioned that cerebellar diaschisis was more pronounced following parietal infarction than infarction of frontal or temporal cortex.

In this study we observed that crossed cerebellar diaschisis occurs commonly following cerebral infarction involving the frontal lobe. Only 3 patients were studied with pure parietooccipital involvement, but cerebellar asymmetry was not observed in these patients. This difference in the incidence of diaschisis between patients with frontal lobe involvement and patients with parietooccipital involvement is significant ($p = 0.007$, Fisher exact test). The extent of contralateral cerebellar depression in CbBF and $CbMRO_2$ was unrelated to the extent of cerebral infarction, as judged by the size of the lesion on the PET scans, or the severity of the motor deficit. Most patients had only mild motor deficits. Finally, there was no relationship between degree of diaschisis and time elapsed since the onset of infarction.

Two additional patients were studied who had reduced $CMRO_2$ and CBF in the distribution of an occluded internal carotid artery in the absence of infarction. This abnormality was reversed following EC-IC bypass. Crossed cerebellar diaschisis was not seen in these patients, suggesting that actual irreversible tissue damage in the cerebral hemisphere is necessary for the development of cerebellar diaschisis and that reversible reductions in metabolism are not sufficient.

Consideration of cerebellar diaschisis provides some useful insights into cerebrocerebellar connections in man. Cerebrocerebellar connections have been re-

viewed in detail elsewhere [1, 4]. Quantitatively, the most important of these connections is the corticopontocerebellar pathway. Tomasch [30] showed that the cerebral peduncle contains 21×10^6 axons, whereas the pyramid contains only 1.1×10^6 axons. About half as many fibers connect with various other brainstem nuclei, leaving 19×10^6 axons on each side as part of the corticopontine system [29]. Virtually all these axons terminate on pontine nuclei that connect mainly to the contralateral cerebellar hemisphere [4]. The corticopontocerebellar system has about forty times the capacity of all other cerebellar afferent sources combined [29]. The cerebellum receives input via pontine nuclei from all major neocortical areas [4], but the relative contributions from different cortical areas and the somatotopic pattern of the projection have not been established in man [33]. Recent work in the rhesus monkey [5, 6] shows that the most dense corticopontine projections arise in the sensorimotor cortex and in parts of the visual cortex. Major contributions also arise in the premotor area (architectonic area 6) and in area 7. Progressively fewer corticopontine projections arise as one moves farther into frontal and temporal association areas. Of importance to the present study is the fact that the major input to the cerebellar hemisphere (crus I and crus II in the monkey) arises in motor and premotor cortex [6]. Somatosensory and parietal association areas provide input to the paramedian lobule, and visual cortex connects to paraflocculus and the superior vermis [5, 6]. Thus, cerebrocerebellar connections to the cerebellar hemispheres are numerous and arise largely from the cortex of the posterior frontal lobe. Our patients with lesions in frontal cortex had depressed $CbMRO_2$ and CbBF in the contralateral cerebellar hemisphere, whereas patients with parietooccipital involvement did not. The lesion was in the posterior frontal lobe, affecting both motor and premotor cortex, in most cases. As noted, these areas are known to project to cerebellar hemisphere in monkeys [5, 6]. Our data are among the first functional evidence for such connections in man. One patient (No. 2) had an anterior frontal infarct, suggesting that some projections to cerebellar hemisphere also arise in this area. The lack of cerebellar diaschisis in patients without frontal lobe involvement is also consistent with Brodal's observation in the monkey [5, 6] that afferents from somatosensory and visual cortex project to more medial regions rather than to crus I and crus II.

Our data also indicate that CbBF and $CbMRO_2$ in the "normal" cerebellar hemisphere (the hemisphere ipsilateral to infarction) are significantly depressed in patients with crossed cerebellar diaschisis, although to a lesser degree than in the opposite side. Furthermore, cerebellar blood flow and metabolism are depressed symmetrically in patients with parietooccipital infarction. Thus, cerebral hemisphere infarction has a generalized effect on the cerebellum unrelated to the site of supratentorial involvement in addition to a specific and more profound effect occurring with frontal infarction.

An alternate interpretation of cerebellar diaschisis is that there is a generalized depression of CbBF and $CbMRO_2$ following infarction in the cerebral hemispheres and that CbBF and $CbMRO_2$ are relatively increased ipsilateral to the cerebral infarction. Increased cerebellar glucose utilization has been observed in animals ipsilateral to observed repetitive limb movements [13, 25]. During PET scanning, however, our patients were resting quietly. In none was any excessive movement of the normal side observed, making this interpretation unlikely.

Our study thus presents one of the first quantitative demonstrations of highly specific changes in cerebellar metabolism and blood flow that result from cerebral infarction. Our results extend to humans the findings of Brodal [5, 6], suggesting that the major cerebral input to the cerebellar hemispheres arises in motor and premotor cerebral cortex. The presence of crossed cerebellar diaschisis in patients with ischemic cerebrovascular disease is evidence of cerebral infarction, as opposed to local metabolic alterations without infarction. As a result, these observations may prove useful in evaluating the importance of metabolic asymmetries of the cerebral hemispheres occurring in other conditions.

Supported in part by Grants HL 13851, NS 14834, and NS 06833 from the National Institutes of Health. Dr Martin is a fellow of the Medical Research Council of Canada.

The authors thank Dr W. T. Thach for helpful discussions; Robert Feldhaus, Lennis Lich, Mark Albertina, John Hood, Jr, Thanh Nha Vu, and the staff of the Washington University Medical School cyclotron for expert technical assistance; and Ms Joyce Parks for secretarial assistance.

References

1. Allen GI, Tsukahara N: Cerebrocerebellar communication systems. Physiol Rev 54:957–1006, 1974
2. Baron JC, Bousser MG, Comar D, Castaigne P: "Crossed cerebellar diaschisis" in human supratentorial brain infarction. Trans Am Neurol Assoc 105:459–461, 1980
3. Baron JC, Bousser MG, Comar D, Duquesnoy N, Sastre J, Castaigne P: "Crossed cerebellar diaschisis": a remote functional depression secondary to supratentorial infarction of man. J Cerebral Blood Flow Metab [Suppl] 1:500–501, 1981
4. Brodal A: Cerebrocerebellar pathways: anatomical data and some functional implications. Acta Neurol Scand [Suppl] 51:153–195, 1972
5. Brodal P: The corticopontine projection in the rhesus monkey: origin and principles of organization. Brain 101:251–283, 1978
6. Brodal P: The pontocerebellar projection in the rhesus monkey: an experimental study with retrograde axonal transport of horseradish peroxidase. Neuroscience 4:193–208, 1979
7. Eichling JO, Raichle ME, Grubb RL Jr, Ter-Pogossian MM:

Evidence of the limitations of water as a freely diffusible tracer in brain of the rhesus monkey. Circ Res 35:358–364, 1974
8. Grubb RL, Raichle ME, Higgins CS, Eichling JO: Measurement of regional cerebral blood volume by emission tomography. Ann Neurol 4:322–328, 1978
9. Hoedt-Rasmussen K, Skinhoj E: Transneural depression of the cerebral hemispheric metabolism in man. Acta Neurol Scand 40:41–46, 1964
10. Hoffman EJ, Huang S-C, Phelps ME: Quantitation in positron emission computed tomography. I. Effect of object size. J Comput Assist Tomogr 3:299–308, 1979
11. Kempinsky WH: Experimental study of distant effects of acute focal brain injury. Arch Neurol Psychiatr 79:376–389, 1958
12. Kempinsky WH, Boniface WR, Keating JBA, et al: Serial hemodynamic study of cerebral infarction in man. Circ Res 9:1051–1058, 1961
13. Kennedy C, Miyaoka M, Suda S, et al: Local metabolic responses in brain accompanying motor activity. Ann Neurol 8:90, 1980
14. Kety SS: The theory and applications of the exchange of inert gas at the lungs and tissues. Pharmacol Rev 3:1–41, 1951
15. Kuhl DE, Phelps ME, Kowell AP, et al: Effects of stroke on local cerebral metabolism and perfusion: mapping by emission computed tomography of ^{18}FDG and $^{13}NH_3$. Ann Neurol 8:47–60, 1980
16. Landau WM, Freygang WH Jr, Roland LP, Sokoloff L: The local circulation of the living brain: values in the unanesthetized and anesthetized cat. Trans Am Neurol Assoc 80:125–128, 1955
17. Lenzi GL, Frackowiak RSJ, Jones T: Regional cerebral blood flow (CBF), oxygen utilization ($CMRO_2$) and oxygen extraction ratio (OER) in acute hemispheric stroke. J Cerebral Blood Flow Metab [Suppl] 1:S504–S505, 1981
18. Mazziotta JC, Phelps ME, Plummer D, Kuhl DE: Quantitation in positron emission computed tomography. V. Physical-anatomical effects. J Comput Assist Tomogr 5:734–743, 1981
19. Melamed E, Lavy S, Portnoy Z: Regional cerebral blood flow response to hypocapnia in the contralateral hemisphere of patients with acute cerebral infarction. Stroke 6:503–508, 1975
20. Meyer JS, Shinohara Y, Kanada T, et al: Diaschisis resulting from acute unilateral cerebral infarction. Arch Neurol 23:241–247, 1970
21. Raichle ME, Grubb RL, Eichling JO, Ter-Pogossian MM: Measurement of brain oxygen utilization with radioactive oxygen-15: experimental verification. J Appl Physiol 40:638–640, 1976
22. Raichle ME, Markham J, Larson K, et al: Measurement of local cerebral blood flow in man with positron emission tomography. J Cerebral Blood Flow Metab [Suppl] 1:19–20, 1981
23. Reivich M: Blood flow metabolism couple in brain. In Plum F (ed): Brain Dysfunction in Metabolic Disorders. Res Publ Assoc Res Nerv Ment Dis 53:125–140, 1974
24. Sakurada O, Kennedy C, Jehle J, et al: Measurement of local cerebral blood flow with iodo[^{14}C]antipyrine. Am J Physiol 234:H59–H66, 1978
25. Schwartzman RJ, Yu J, Alexander GM, et al: Quantitative 2-deoxyglucose mapping of the cerebellum. Ann Neurol 6:165–166, 1979
26. Slater R, Reivich M, Goldberg H, et al: Diaschisis with cerebral infarction. Stroke 8:684–690, 1977
27. Ter-Pogossian MM, Eichling JO, Davis DO, Welch MJ: The measure in vivo of regional cerebral oxygen utilization by means of oxyhemoglobin labelled with radioactive oxygen-15. J Clin Invest 49:381–391, 1970
28. Ter-Pogossian MM, Ficke DC, Hood JT, et al: PETT VI: a positron emission tomograph utilizing cesium fluoride scintillation detectors. J Comput Assist Tomogr 6:125–133, 1982
29. Tomasch J: The overall information carrying capacity of the major afferent and efferent cerebellar cell and fiber systems. Confin Neurol 30:359–367, 1968
30. Tomasch J: The numerical capacity of the human cortico-ponto-cerebellar system. Brain Res 13:476–484, 1969
31. Urich H: Malformations of the nervous system, perinatal damage and related conditions in early life. In Blackwood W, Corsellis JAN (eds): Greenfield's Neuropathology. Third edition. London, Arnold, 1976, p 401
32. von Monakow C: Die Lokalisation im Grosshirn und der Abbau der Funktion durch kortikale Herde. Wiesbaden, Bergmann, 1914
33. Williams PL, Warwick R: Functional Neuroanatomy of Man. Edinburgh, Churchill Livingstone, 1975
34. Yamamoto M, Ficke DC, Ter-Pogossian MM: Performance study of PETT VI, a positron computed tomograph with 288 cesium fluoride detectors. IEEE Trans Nuclear Sci NS-29:529–533, 1982